MAPKs Modulate RPE Response to Oxidative Stress

Zhaohui Wang

Gradalis, Inc., 1700 Pacific Ave., Suite 1100, Dallas, Texas, 75201, USA
vwang@gradalisbio.com

Thomas J. Bartosh[1], Min Ding[2], and Rouel S. Roque[3]

[1]Texas A&M HSC, Institute for Regenerative Medicine at Scott & White Hospital, Temple, TX 76502 USA;
[2]Dept. of Integrative Physiology, University of North Texas HSC, Fort Worth, Texas 76107 USA; and
[3]Dept. of Basic Sciences, Touro University Nevada, Henderson NV 89014 USA
bartosh@medicine.tamhsc.edu; min.ding@unthsc.edu; rouel.roque@tun.touro.edu

Abstract—**To investigate the role of mitogen-activatedprotein kinases (MAPK) in the response of the retinal pigment epithelium (RPE) to oxidative stress (OS), a well-characterized RPE cell line (ARPE-19) was exposed to an oxidant-generating system catalyzed by glucose oxidase and glucose (GO/G). ARPE-19 cells were characterized for morphological changes, mitochondrial membrane permeability (MMP), and cell survival following exposure to GO/G. The effects of GO/G on MAPK activity were determined by assaying for p38MAPK expression and activity in the presence or absence of SB203580, a specific p38MAPK inhibitors, or p38MAPK siRNA. ARPE-19 cells exposed to GO/G showed morphological changes, increased MMP, and cell death. Exposure to OS promoted increased phosphorylation of p38MAPK and hsp27, a downstream target of p38MAPK. SB203580, but not p38 MAPK siRNA, inhibited ARPE-19 cell death. In conclusion, activation of p38MAPK may promote downstream pathways responsible for the morphological changes observed in RPE cells during oxidative damaging, however, these pathways do not appear to be responsible for OS-induced RPE degeneration.**

Index Terms—**oxidative stress, retinal pigment epithelium, mitogen activated protein kinases, p38MAPK, age-related macular degeneration, reactive oxygen species**

I. INTRODUCTION

Age-related macular degeneration (AMD), leading cause of permanent blindness in the United States, is characterized by progressive degeneration of the retinal-pigment epithelium (RPE) and neighboring photoreceptors in the retina. This often leads to severe visual impairment and permanent blindness [1], [2].

According to epidemiological studies, 11% of 65-74 years old people have AMD, with the incidence rising to 28% in people aged 75-85. About 2% of elderly suffer from blindness due to AMD [3]. It is estimated that the incidence will increase 50% by 2020 [4]. In spite of the downstream signaling pathways including hsp27, these advances in medicine, the treatment of AMD also remains unsatisfactory.

Although the visual loss results from the loss of photoreceptor cells, the initial pathogenesis most likely involves degeneration and atrophy of RPE. The progressive RPE dysfunction and eventual RPE cell death cause subsequent degeneration of rod and cone photoreceptors, perhaps due to loss of trophic support and defense barrier. Oxidative stress has been acknowledged as a leading cause of the degenerative changes, but the exact role of reactive oxygen species (ROS) in this disease remains to be established. Moreover, while mitogen-activated protein kinases (MAPKs) are suggested to be involved in oxidative stress-induced RPE degeneration, the precise functions and molecular mechanisms of MAPKs in RPE degeneration remain elusive [5-7]. The goal of this study is to establish an oxidative stress-induced RPE degeneration model and elucidate the role of MAPKs in RPE cell death.

In this study, a well-characterized RPE cell line (ARPE-19) was exposed to a glucose-based oxidant-generating system catalyzed by glucose oxidase (GO/G). ARPE-19 cells were characterized for morphological changes, mitochondrial membrane permeability (MMP), and cell survival following prolonged exposure to GO/G. The effects of OS on MAPK activity were determined by assaying for p38MAPK expression and activity in the presence or absence of pharmacological inhibitors or siRNA.

II. MATERIALS AND METHODS

A. Reagents

Calcein AM, ethidium homodimer-1, $H_2DCFH-DA$, JC-1, Rhodamine-phallodin, and Alexa-conjugated secondary antibodies were obtained from Invitrogen (Carlsbad, CA). Anti-phospho-p38 MAPK antibody and the Cell Titer 96 Aqueous Cell Proliferation Assay (MTS) kit was obtained from Promega (Madison, WI). SB203580 was purchased from Calbiochem (EMD

Biosciences, San Diego, CA) while p38 MAPK siRNA and antibodies against p38 MAPK, hsp27, and phospho-hsp27 were from Cell Signaling (Danvers, MA). Glucose oxidase, D-glucose, and N-Acetyl Cysteine were obtained from Sigma (St. Louis, MO).

B. Cell Culture

A spontaneously transformed human retinal pigment epithelial cell line, ARPE-19 cells was used in this study. ARPE-19 cells maintain the major characteristics of RPE cells including expression of specific cell markers, tight junction formation, and retinoid metabolism [8]. ARPE-19 cells were maintained in growth medium (Dulbecco's modified Eagle's medium, 10% fetal bovine serum, 2 mM L-glutamine, 100 units/ml penicillin, 100 mg/ml streptomycin, and 15 mM HEPES buffer) at 37℃ in a humidified atmosphere of 5% CO2 and 95% air.

C. In Vitro Model for Oxidative Stress

To investigate the effects of oxidative stress on the RPE, ARPE-19 cells were exposed to a glucose-based oxidant-generating system catalyzed by glucose oxidase (GO/G). Glucose oxidase catalyzes the oxidation of β-D-glucose to D-glucono-1,5-lactone and hydrogen peroxide, using molecular oxygen as the electron acceptor.

ARPE-19 cells were plated in growth medium then transferred to glucose-free serum-free medium for 24h. The following day, cells were exposed to 0-30mU/ml glucose oxidase in the presence of 1 g/L glucose for 0-5h.

To determine oxidative stress on RPE cells, the generation of intracellular reactive oxygen species (ROS) following GO/G treatment was measured using the fluorescent dye H_2DCFH-DA. ARPE-19 cells were pre-loaded with $10\mu M$ H_2DCFH-DA for 30 minutes at 37℃. The unbound H_2DCFH-DA was washed off and cells were treated with GO/G. H_2DCFH-DA fluorescence was detected using a fluorescent microplate reader (model FL600; Biotek, Highland Park, VT). Readings were normalized to the untreated control groups.

D. Cell Survival Assay

ARPE-19 cells plated on 96-well plates at $4X10^3$ cells/well and treated with GO/G for 0-6hr were washed with serum-free DMEM and incubated with 2mM calceinAM and 4mM ethidium homodimer at 37°C for 30min. Cells were observed and images captured under a fluorescence microscope.

To measure the amount of cell death, ARPE-19 cells were incubated for 1h with MTS reagent (3-4,5-dimethylthiazol-2-yl)-5-(3-carboxymethosyphenyl)-2-(4 sulfophenyl) -2H-tetrazolium) that is converted to a water-soluble formazan by dehydrogenase enzyme found in metabolically active cells. The quantity of formazan product was measured using a microplate reader at 490nm. A standard curve was prepared for each set of experiments using 1.25-50 $\times10^3$cells/well. Experiments were done at least three times.

E. Mitochondrial Membrane Permeability

ARPE-19 cells were seeded in 96-well plate overnight and washed twice with serum-free growth medium. After overnight incubation, the cells were treated with GO/G, washed once with HBSS buffer, then incubated with 1 μg/mL JC-1 and 0.1% DMSO at 37 °C for 20min. Afterwards, cells were kept on ice, washed twice with ice-cold DPBS, and overlaid with phenol red-free medium. Cells were examined and images were captured on a Nikon microphot FXA microscope with epifluorescent attachment (Nikon Corp., Tokyo, Japan).

F. Immunocytochemistry

ARPE-19 cells were plated on 8-well Lab-Tek chamber slides and fixed with 2% paraformaldehyde for 20 minutes following treatment. Fixed cells were permeabilized with 0.05% saponin in phosphate buffered saline (PBS; 10mM phosphate [pH 7.4], 150mM NaCl) for 15 minutes, blocked in 0.5% BSA and 4% normal goat serum for 1 hour, and processed for immunostaining as previously published. Appropriate controls involved substituting primary antibodies with mouse or rabbit IgG. Cell nuclei were counterstained with DAPI.

G. Western Blot Assay

Lysates separated by SDS-PAGE were transferred to nitrocellulose membrane at 100V. Membranes were blocked with 5% non-fat dried milk for 1h and processed for Western blotting as previously published. Reactions were visualized using luminol reagent.

H. siRNA Knockdown

ARPE-19 cells were seeded at a density of 15,000mcells/cm^2 in 12-well plates overnight, then transfected with 20 nM p38MAPK siRNA. Briefly, 20nM siRNA and 2ul transfection reagent were added to serum-free growth medium and equilibrated to room temperature for 5 minutes. 100ul of the combined solution was added to the cells. 24 hours post-transfection, ARPE-19 cell were transferred to growth medium and incubated for another 24 hours prior to indicated treatment. A fluorescein-labeled non-targeted siRNA was used as control to monitor transfection efficiency.

III. RESULTS

A. GO/G-Induced RPE Cell Death Is Dose-Dependent

To characterize the cell death and optimize the experimental parameters in this RPE degeneration model, we determined whether the effects of lethal oxidative stress on RPE cells were dose-dependent using MTS assay. In dose-response experiments, ARPE-19 cells were exposed to 0-30mU/ml glucose oxidase plus 1g/L glucose (GO/G) for 0-5 hours. There was no decrease of cell viability observed with exposure to 0-15 mU/ml GO/G for 5 hours. At 20mU/ml GO/G, there was 40% loss of cell viability, while most of the cells were dead when exposed to 25 and 30 mU/ml GO/G (Fig. 1A). Moreover, cells exposed to 25 mU/ml GO/G remained viable for 0-3 hours, with only ~40% survival after 4 hours of treatment (Fig. 1B).
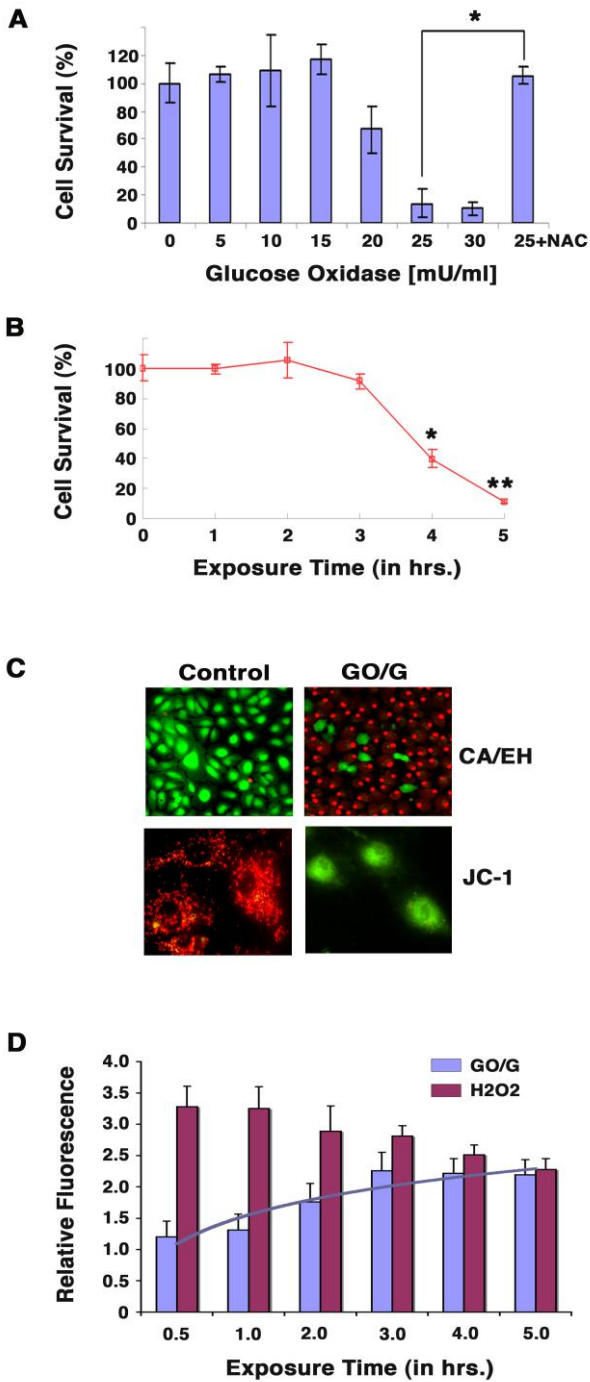
B. GO/G Induces Cell Death and MMP Depolarization

GO/G for 4 hours and treated with calcein AM and ethidium homodimer to visualize live or dead cells, respectively. Injured ARPE-19 cells demonstrated nuclear DNA shrinkage, different from DNA fragmentation typical of apoptosis. Since oxidative injured RPE cells did not exhibit typical apoptotic characteristics, we tested potential changes in the mitochondrial membrane potential (MMP) using JC-1 to determine mitochondrial membrane integrity. ARPE-19 cells were treated by 25mu/ml GO/G for 5 hours and JC-1 fluorescence was quantitatively measured by a fluorescent microplate reader. After treatment with 25mU/ml GO/G, there was significant increase in green staining of damaged mitochondria, along with decreased red staining of healthy mitochondria (Fig. 1C).

C. GO/G Generates ROS

Glucose oxidase catalyzes the production of hydrogen oxide using glucose and water as substrates. To measure the intracellular reactive oxygen species (ROS produced by glucose oxidase/glucose, the fluorescent dye $H_2DCFH-DA$ was employed in this study. In addition, we compared the generation pattern of ROS between GO/G and hydrogen peroxide. When ARPE-19 cells were treated with hydrogen peroxide, there was an acute and significant increase of ROS fluorescence at half an hour, followed by gradual dissipation of ROS with time (Fig. 1D). In contrast, when ARPE-19 cells were treated with GO/G, the production of ROS increased gradually and lasted 6 hours. Our study suggests that GO/G induces gradual generation of reactive oxygen species, which may resemble the long-term accumulation of oxidative stress in AMD patients.

D. Oxidative Stress Induces Cytoskeletal Remodeling

Figure 1. Oxidative stress-induced cell death and depolarization of mitochondrial membrane potential in ARPE-19 cells. A, B: ARPE-19 cells were exposed to glucose oxidase (0-30 mU/ml) plus 1g/L glucose for 0-5 hours. 2mM ROS scavenger N-Acetylcysteine (NAC) was used to inhibit cell death. Cell survival was examined by MTS assay. C: ARPE-19 cells were exposed to 25mU/ml glucose oxidase plus 1g/L glucose for 0 -5 hours and labeled with calcein AM (CA) and ethidium homodimer (EH) for viability or JC-1 for MMP. D: ROS generated by cells exposed to GO/G were compared with those treated with 2 mM H2O2 using a fluorescent dye, H₂DCFH-DA. Experiments were done in triplicates (n=3) and analyzed by Students't-test. Data represent mean ±SD.
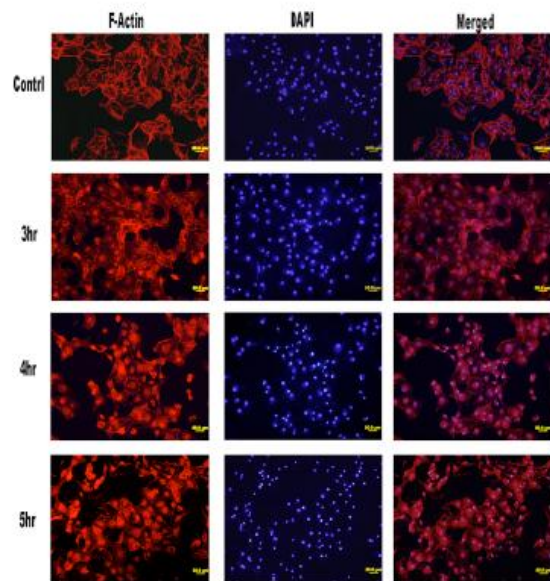

Figure 2. Prolonged exposure to oxidative stress induces cytoskeletal remodeling. ARPE-19 cells were exposed to 25mU/ml glucose oxidase plus 1g/L glucose for 0-5 hours, then stained with Rhodamine-phallodin to label filamentous actin. DAPI was used to counterstain the nucleus.

To characterize the effects of oxidative injury on nuclear DNA, ARPE-19 cells were exposed to 25mU/ml

It is well established that oxidative stress induces cytoskeletal reorganization during cell death. To characterize the changes in the actin cytoskeleton, ARPE-19 cells were treated with 25mU/ml glucose oxidase plus 1g/L glucose for 0-5 hours and labeled with Rhodamine phallodin to stain filamentous actin. GO/G treated-cells displayed morphological changes within 2-3 hours of treatment. Actin filaments re-organized around the nucleus in contrast to their distribution in the periphery of untreated cells (Fig. 2). Small rounded particles stained for actin appeared to be exosomes released by RPE cells (data not shown). To confirm this observation, we performed similar treatment using calcein AM, which identified live cells. Small round calcein AM-labeled particles were localized in the plasma membrane of live RPE cells similar to the above. Our findings suggest that oxidative stress promotes early cytoskeleton remodeling and perhaps membrane blebbing in RPE cells, which could contribute to drusen formation reported in AMD.

E. Oxidative Stress Promotes Activation and Nuclear Translocation of p38MAPK

To determine the role of p38MAPK signaling in RPE cells exposed to oxidative damage, the expression of activated p38MAPK was examined at various time points following exposure to 25mU/ml GO/G in immunoblots. p38MAPK was activated with 30 min. and peaked at 2-3 hours post-treatment. Activated p38MAPK levels were maintained above basal level even after 5 hours of treatment (Fig. 3A).
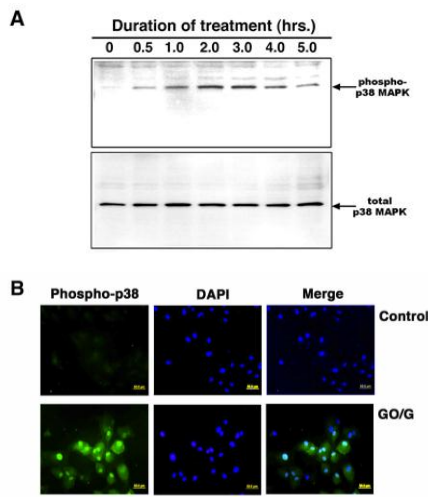

Figure 3. Oxidative stress promotes p38MAPK activation and nuclear translocation. A, ARPE-19 cells were exposed to 25 mU/ml glucose oxidase plus 1g/L glucose for indicated periods of time and the activation of p38 MAPK was examined by immunoblotting. Total p38MAPK was used as loading control. B, ARPE-19 was exposed to the same treatment for 3 hours and the distribution of activated p38MAPK was determined by immunocytochemistry using anti-phospho-p38MAPK antibody. DAPI was used to counterstain the nucleus.

To determine the cellular distribution of p38MAPK, we examined the expression of the phosphorylated p38 MAPK by immunostainning. ARPE-19 cells were exposed to oxidative stress for 3 hours and processed for labeling with an anti-phospho-p38MAPK antibody. Significant accumulation of activated p38MAPK was observed in the nucleus in contrast to non-detectable nuclear staining in untreated cells. Furthermore, the expression of activated p38MAPK was also increased in the cytoplasm, consistent with previous observations in immunoblots (Fig. 3B).

F. SB203580 Promotes Survival during Oxidative Stress

To further explore the function of p38MAPK in RPE degeneration, we used SB203580, a widely reported specific pharmacological inhibitor of p38MAPK, to block p38MAPK activity. ARPE-19 cells were pretreated with 5-20um SB203580 for 2 hours and subjected to 25mU/ml GO/G for 5 hours. Cell viability was measured by either MTS assay or calcein AM/ethidium homodimer staining. SB203580 inhibited ARPE-19 cell death from GO/G-induced oxidative stress in a dose-dependent manner (Fig. 4A). Increased calcein AM staining and decreased ethidium homodimer labeling was consistent with the apparent protective effect of SB203580 against oxidative stress (Fig. 4B).
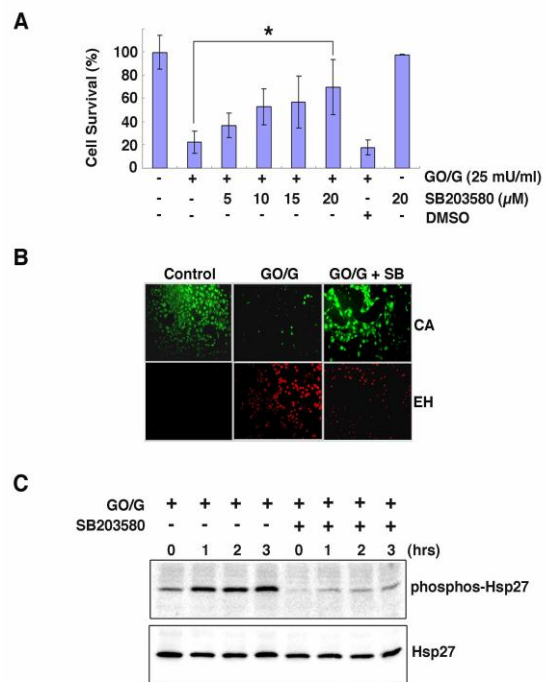

Figure 4. p38 MAPK inhibitor, SB203580, suppresses oxidative stress-induced cell death and blocks the activation of hsp27. ARPE-19 cells were exposed to 25mU/ml glucose oxidase plus 1g/L glucose for 5 hours in the presence of SB203580 at different concentrations (5-20uM). After overnight recovery, the cell viability was measured by MTS assay (A), or by staining with 2uM calcein AM and 4uM ethidium homodimer for 20mins (B), and tested for hsp27 activation using immunoblotting and a phospho-hsp27 antibody (C). Hsp27 staining was used as loading control. Experiments were done in triplicates (n=3) and analyzed by Students't-test. Data represent mean ±SD.

G. SB20358 Blocks p38MAPK-Mediated hsp27 Activation

In addition to regulating nuclear substrates, such as transcription factors, p38MAPK exerts its effects by

activating cytoplasmic substrates. For example, p38 MAPK activates heat shock protein 27 (hsp27) and hence regulates cytoskeleton remodeling during apoptosis or differentiation. In this study, ARPE-19 cells were exposed to 25mU/ml GO/G for indicated period of time in the presence or absence of SB203580, and tested for activation of hsp27 using immunoblotting. Hsp27 was activated with increased duration of treatment, consistent with the activation pattern of p38MAPK (Fig. 4C). Furthermore, hsp27 phosphorylation was inhibited by SB203580. These results demonstrate that oxidative stress induces activation and nuclear accumulation of p38MAPK, which promoted downstream activation of hsp27.

H. p38MAPK Knockdown Does not Inhibit Oxidative Stress-Induced RPE Cell Death

To further verify the role of p38MAPK in RPE degeneration, we utilized p38MAPK siRNA to interfere with protein expression of p38MAPK. Briefly, ARPE-19 cells were transfected with either p38MAPK siRNA or control siRNA for 48 hours. Transfected cells were harvested and the expression of p38MAPK was determined by immunoblotting. p38MAPK expression was significantly suppresed compared with the control group (Fig. 5A). However, siRNA-transfected cells exposed to oxidative stress did not survive the oxidative insult similar to cells transfected with control siRNA. No statistical difference between the p38MAPK knockdown group and control group was observed (Fig. 5B). Our findings argue against a role for p38MAPK in oxidative stress induced- RPE cell death.

IV. DISCUSSION

In the aging retina, oxidative stress and reactive oxygen species (ROS) have been hypothesized to play a major factor in the pathogenesis of AMD [2]. To simulate oxidative stress in vitro, a variety of oxidants have been employed to induce oxidative stress to RPE cells [9-12]. Both hydrogen peroxide and t-terbutyl peroxide are broadly used to elicit oxidative stress and induce RPE cell death. However, most of the oxidants promote immediate changes and decrease with time, a pattern different from the chronic increase in amounts ROS expected in during oxidative insult. Furthermore, in order to induce RPE cell death, high concentrations of hydrogen peroxide often have to be used, usually beyond physiological levels [12]. To mimic the progressive and long term ROS production and subsequent RPE degeneration observed in AMD, we utilized a glucose oxidase/glucose (GO/G) system to continuously generate hydrogen peroxide. GO/G has been used to induce oxidative stress both extracellularly and intracellularly in a variety of cell culture models [13-19]. Furthermore, glucose oxidase has been successfully delivered into animals to elicit oxidative stress in lung endothelial cells [20].

Oxidative stress induces membrane blebbing and cytoskeleton remodeling as part of the defense response of RPE cells to oxidative damage. A cell sheds off part of its membrane and cytoplasm to discard damaged plasma membranes, cellular organelles, or macromolecules following lipid peroxidation. Histopathological studies of human AMD specimens or animal models suggest that membrane blebbing of RPE cells in response to oxidative damage probably result in exosome formation that contribute to drusen accumulation, a characteristic sign of early AMD [21]. Several *in vitro* studies have been employed to induce membrane blebbing to investigate the composition of shed membrane particles and the molecular composition of drusen [21], [22]. Our studies showed that ROS generated from the GO/G reaction result in cytoskeleton remodeling and membrane blebbing characteristic of oxidative damage.
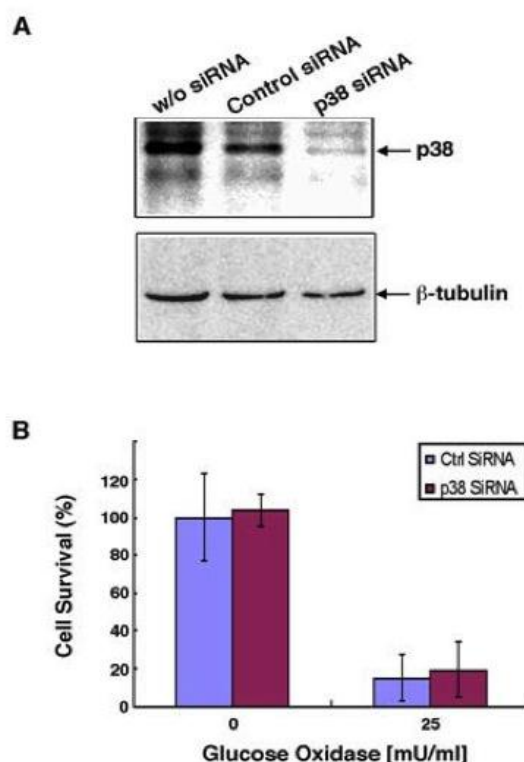

Figure 1. Knock down p38 MAPK gene expression does not suppress glucose oxidase/glucose-induced RPE cell death. A. ARPE-19 cells were transiently transfected with both p38 MAPK siRNA and control SiRNA and tested for expression of p38 MAPK by immunoblotting. β-tubulin was used as loading control. **B:** ARPE-19 cells transfected with SiRNA were exposed to 25mU/ml glucose oxidase plus glucose for 5 hours. After overnight recovery, the cell survival was measured by MTS assay. Experiments were done in triplicates (n=3) and analyzed by Student's-test. Data represent mean ±SD.

Prolonged exposure of the ARPE-19 cell lead to lethal oxidative injury caused cell death in a dose-dependent and time-dependent manner. However, morphogical changes in the cells were different from those reported in classical apoptosis involving DNA fragmentation. ARPE-19 cells exposed to GO/G displayed DNA condensation but not fragmentation. A similar observation has been reported in caspase-independent PARP cleavage and AIF translocation to the nucleus during cell death [23].

The integrity of mitochondria is crucial for cells to maintain physiological functions. In apoptosis, depolarized mitochondria releases apoptotic proteins, such as cytochrome C and apoptosis-inducing factor (AIF), initiate the caspase cascade and subsequent DNA fragmentation [24]. Mitochondrial membrane potential depolarization is a hallmark of apoptosis, but it has also been shown in early phases of necrosis [24], [25]. In our study, mitochondrial membrane potential depolarization was observed in oxidative damaged RPE cells in the absence of other signs of apoptosis. Our study suggests that glucose oxidase/glucose induces RPE degeneration with characteristics of early changes of cytoskeleton remodeling and membrane blebbing that could contribute to drusen formation; followed by depolarization of mitochondrial membrane potential and DNA condensation without fragmentation, consistent with atypical RPE cell death observed during oxidative damage and AMD.

In this study, also we investigated the molecular mechanism likely responsible for oxidative stress-induced RPE cell death. Initially, we tested the effects of a wide array of pharmacological inhibitors to established signaling pathways on RPE cell death and found SB203580, an inhibitor of p38MAPK, solely effective in rescuing RPE cells from GO/G-induced oxidative damage [data not shown].

In response to environmental stresses, p38MAPK may stimulate [26], [27] or protect [28] [29] against cell death. Interestingly, the role of p38MAPK in regulating cell death or survival is dependent on specific cell type, stimulus, or p38MAPK isoform involved in the process. p38MAPKβ may attenuate the cell death induced by Fas ligation and UV irradiation, whereas p38MAPKα promotes cell death [28]. p38MAPK has also been suggested to induce RPE cell death in response to oxidative stress. For instance, lethal hydrogen peroxide activated p38MAPK and promoted cell death, both of which were inhibited by SB203580 [5]. However, p38MAPK has also been reported to protect RPE cells from oxidative damage in other studies utilizing the same ARPE-19 cell line.

SB203580 is a specific p38MAPK inhibitor and extensively used to inhibit the activity of both p38MAPKα and p38MAPKβ and p38MAPK-mediated cell death. However, recent findings challenge the specificity of SB203580. For example, SB20350 could directly bind and activate Raf and MEK upstream of p42/44 MAPK. SB203580 was shown to activate Raf-1 in a dose-dependent mode in quiescent smooth muscle cells [30], erythroleukaemic cells [31], rabbit aortic vascular smooth muscle cells [32], THP-1 monocytic cells and U937 cells [33]. In 3T3 cells and 293 cells, SB203580 at micromolar concentrations activated both c-Raf and MEK1 independent of p38MAPK inhibition [34]. Hence, activation of the Raf-MEK-p42/p44MAPK pathway, and not inhibition of the p38MAPK pathway, may be responsible for the protective effect of SB203580 on GO/G-treated ARPE-19 cells. Moreover, interference with p38MAPK siRNA did not block RPE cell death,

consistent with this idea. Preliminary data in our lab shows direct stimulation of the p42/p44MAPK pathway by SB203580.

Heat shock protein 27 (hsp27) is a specific substrate of p38MAPK and regulates cytoskeleton reorganization in response to environmental stresses [35]. In our study, hsp27 was activated by GO/G-induced oxidative stress and the activation of hsp27 was inhibited by p38MAPK inhibitor, suggesting that p38MAPK may be involved in hsp27-mediated cytoskeleton remodeling and membrane blebbing. Clearly, additional studies are needed to investigate whether p38MAPK signaling via hsp27 could be involved in drusen formation in AMD.

REFERENCES

[1] J. Cai, K. C. Nelson, M. Wu, P. Sternberg, Jr and D. P. Jones, "Oxidative damage and protection of the RPE," *Prog. Retin. Eye Res*, vol. 19, pp. 205-221, 2000.

[2] Y. Imamura, *et al*. "Drusen, choroidal neovascularization, and retinal pigment epithelium dysfunction in SOD1-deficient mice: A model of age-related macular degeneration," in *Proc. Natl. Acad. Sci. U. S. A.*, vol. 103, 2006, pp. 11282-11287.

[3] N. Congdon, *et al*. "Causes and prevalence of visual impairment among adults in the United States," *Arch. Ophthalmol*, vol. 122, pp. 477-485, 2004.

[4] D. S. Friedman, *et al*. "Prevalence of age-related macular degeneration in the United States," *Arch. Ophthalmol*, vol. 122, pp. 564-572, 2004.

[5] T. C. Ho, *et al*. "Activation of mitogen-activated protein kinases is essential for hydrogen peroxide-induced apoptosis in retinal pigment epithelial cells," *Apoptosis*, vol. 11, pp. 1899-1908, 2006.

[6] N. Strunnikova, *et al*. "Survival of retinal pigment epithelium after exposure to prolonged oxidative injury: A detailed gene expression and cellular analysis," *Invest. Ophthalmol. Vis. Sci.* vol. 45, pp. 3767-3777, 2004.

[7] A. L. Glotin, *et al*. "Sustained versus transient ERK1/2 signaling underlies the anti- and proapoptotic effects of oxidative stress in human RPE cells," *Invest. Ophthalmol. Vis. Sci.* vol. 47, pp. 4614-4623, 2006.

[8] K. C. Dunn, A. E. Aotaki-Keen, F. R. Putkey, and L. M. Hjelmeland, "ARPE-19, a human retinal pigment epithelial cell line with differentiated properties," *Exp. Eye Res,* vol. 62, pp. 155-169, 1996.

[9] P. Yang, J. J. Peairs, R. Tano, and G. J. Jaffe, "Oxidant-mediated Akt activation in human RPE cells," *Invest. Ophthalmol. Vis. Sci.* vol. 47, pp. 4598-4606, 2006.

[10] J. Cai, M. Wu, K. C. Nelson, Jr. P. Sternberg, and D. P. Jones, "Oxidant-induced apoptosis in cultured human retinal pigment epithelial cells," *Invest. Ophthalmol. Vis. Sci.* vol. 40, pp. 959-966, 1999.

[11] G. F. Jin, J. S. Hurst, and B. F. Godley, "Hydrogen peroxide stimulates apoptosis in cultured human retinal pigment epithelial cells," *Curr. Eye Res.* vol. 22, pp. 165-173, 2001.

[12] T. K. Garg and J. Y. Chang, "Oxidative stress causes ERK phosphorylation and cell death in cultured retinal pigment epithelium: prevention of cell death by AG126 and 15-deoxy-delta 12, 14-PGJ2," *BMC Ophthalmol.* vol. 3, pp. 5, 2003.

[13] Y. S. Kim and S. U. Kim, "Oligodendroglial cell death induced by oxygen radicals and its protection by catalase," *J. Neurosci. Res.* vol. 29, pp. 100-106, 1991.

[14] A. Dhanasekaran, *et al*. "Supplementation of endothelial cells with mitochondria-targeted antioxidants inhibit peroxide-induced

mitochondrial iron uptake, oxidative damage, and apoptosis," *J. Biol. Chem.* vol. 279, pp. 37575-37587, 2004.

[15] G. U. Bae, *et al.* "Hydrogen peroxide activates p70(S6k) signaling pathway," *J. Biol. Chem.* vol. 274, pp. 32596-32602, 1999.

[16] J. Y. Song, J. W. Lim, H. Kim, T. Morio, and K. H. Kim, "Oxidative stress induces nuclear loss of DNA repair proteins Ku70 and Ku80 and apoptosis in pancreatic acinar AR42J cells," *J. Biol. Chem.* vol. 278, pp. 36676-36687, 2003.

[17] S. Mueller, K. Pantopoulos, C. A. Hubner, W. Stremmel, and M. W. Hentze, "IRP1 activation by extracellular oxidative stress in the perfused rat liver," *J. Biol. Chem.* vol. 276, pp. 23192-23196, 2001.

[18] G. Corna, P. Santambrogio, G. Minotti, and G. Cairo, "Doxorubicin paradoxically protects cardiomyocytes against iron-mediated toxicity: role of reactive oxygen species and ferritin," *J. Biol. Chem.* vol. 279, pp. 13738-13745, 2004.

[19] A. J. Gow, *et al.* "Immunotargeting of glucose oxidase: Intracellular production of H(2)O(2) and endothelial oxidative stress," *Am. J. Physiol.* vol. 277, pp. 271-81, 1999.

[20] M. Christofidou-Solomidou, *et al.* "Immunotargeting of glucose oxidase to endothelium in vivo causes oxidative vascular injury in the lungs," *Am. J. Physiol. Lung Cell. Mol. Physiol.* vol. 278, pp. 794-805, 2000.

[21] W. R. Green, "Histopathology of age-related macular degeneration," *Mol. Vis.* vol. 5, pp. 27, 1999.

[22] N. Strunnikova, *et al.* "Regulated heat shock protein 27 expression in human retinal pigment epithelium," *Invest. Ophthalmol. Vis. Sci.* vol. 42, pp. 2130-2138, 2001.

[23] C. Zhang, J. Baffi, S. W. Cousins, and K. G. Csaky, "Oxidant-induced cell death in retinal pigment epithelium cells mediated through the release of apoptosis-inducing factor," *J. Cell. Sci.* vol. 116, pp. 1915-1923, 2003.

[24] G. Kroemer, B. Dallaporta, and M. Resche-Rigon, "The mitochondrial death/life regulator in apoptosis and necrosis," *Annu. Rev. Physiol,* vol. 60, pp. 619-642, 1998.

[25] J. G. Pastorino, G. Simbula, E. Gilfor, J. B. Hoek, and J. L. Farber, "Protoporphyrin IX, an endogenous ligand of the peripheral benzodiazepine receptor, potentiates induction of the mitochondrial permeability transition and the killing of cultured hepatocytes by rotenone," *J. Biol. Chem.* vol. 269, pp. 31041-31046, 1994.

[26] S. Zhuang, J. T. Demirs, and I. E. Kochevar, "P38 mitogen-activated protein kinase mediates bid cleavage, mitochondrial dysfunction, and caspase-3 activation during apoptosis induced by singlet oxygen but not by hydrogen peroxide," *J. Biol. Chem.* vol. 275, pp. 25939-25948, 2000.

[27] H. Shimizu, *et al.* "Activation of p38 mitogen-activated protein kinase and caspases in UVB-induced apoptosis of human keratinocyte HaCaT cells," *J. Invest. Dermatol.* vol. 112, pp. 769-774, 1999.

[28] S. Nemoto, J. Xiang, S. Huang, and A. Lin, "Induction of apoptosis by SB202190 through inhibition of p38beta mitogen-activated protein kinase," *J. Biol. Chem.* vol. 273, pp. 16415-16420, 1998.

[29] I. Dalle-Donne, R. Rossi, A. Milzani, P. Di Simplicio, and R. Colombo, "The actin cytoskeleton response to oxidants: from small heat shock protein phosphorylation to changes in the redox state of actin itself," *Free Radic. Biol. Med.* vol. 31, pp. 1624-1632, 2001.

[30] A. Kalmes, J. Deou, A. W. Clowes, and G. Daum, "Raf-1 is activated by the p38 mitogen-activated protein kinase inhibitor, SB203580," *FEBS Lett.* vol. 444, pp. 71-74, 1999.

[31] K. U. Birkenkamp, *et al.* "The p38 MAP kinase inhibitor SB203580 enhances nuclear factor-kappa B transcriptional activity by a non-specific effect upon the ERK pathway," *Br. J. Pharmacol.* vol. 131, pp. 99-107, 2000.

[32] S. Fatima, Z. Khandekar, J. H. Parmentier, and K. U. Malik, "Cytosolic phospholipase A2 activation by the p38 kinase inhibitor SB203580 in rabbit aortic smooth muscle cells," *J. Pharmacol. Exp. Ther.* vol. 298, pp. 331-338, 2001.

[33] S. Numazawa, *et al.* "Regulation of ERK-mediated signal transduction by p38 MAP kinase in human monocytic THP-1 cells," *J. Biochem. (Tokyo),* vol. 133, pp. 599-605, 2003.

[34] Y. Ishii, S. Sakai, and Y. Honma, "Pyridinyl imidazole inhibitor SB203580 activates p44/42 mitogen-activated protein kinase and induces the differentiation of human myeloid leukemia cells," *Leuk. Res.* vol. 25, pp. 813-820, 2001.

[35] M. de Graauw, *et al.* "Heat shock protein 27 is the major differentially phosphorylated protein involved in renal epithelial cellular stress response and controls focal adhesion organization and apoptosis," *J. Biol. Chem.* vol. 280, pp. 29885-29898, 2005.

Zhaohui Wang, Ph.D. is a Research Associate at the Gradalis, Inc., Dallas, Texas, U.S.A. He completed his B.S. and M.S. degrees in Biopharmaceutics at the China Pharmaceutical University in Nanjing, China. Following graduation, he worked briefly in various capacities with several pharmaceutical companies in China till 2001 when he was accepted into the Ph.D. program in Biomedical Sciences at the University of North Texas Health Science Center at Fort Worth, Texas. He spent his first two years in the laboratory of Patrick Cammarata, Ph.D. and later joined the laboratory of Rouel S. Roque, M.D. to work on stem cells and retinal degeneration. He completed his Ph.D. in Biomedical Sciences at the University of North Texas Health Science Center at Fort Worth, Texas in 2007, and successfully passed the Foreign Pharmacy Graduate Equivalency Examination. In 2007, Dr. Wang accepted a research position at Gradalis Inc., a biotech company involved in the development of cancer therapeutics, where he remains to date.

Thomas J. Bartosh, Ph.D. is an Instructor of Molecular and Cellular Medicine at the Institute for Regenerative Medicine located in Temple, Texas, U.S.A. He received a B.S. degree in Biology from The University of Texas Arlington in 2002. Then, in 2008, he earned his Ph.D. degree in Cell Biology and Genetics from The University of North Texas Health Science Center working with Rouel S. Roque, M.D. on the molecular regulation of cardiac stem cell growth and differentiation in 3D cardiac micro-tissue models. Dr. Bartosh joined the Texas A&M University System Health Science Center as a post-doctoral fellow in 2008 working in the laboratory of Dr. Darwin J. Prockop to develop therapies with mesenchymal stem cells from the bone marrow. In 2011, he accepted a position as supervisor of the flow cytometry/cell sorting core laboratory at the Institute for Regenerative Medicine. Dr. Bartosh joined the faculty of Texas A&M Health Science Center in 2012.

Rouel S. Roque, M.D. is a Professor of Basic Science and the Director of Anatomy at Touro University Nevada in Henderson, Nevada, U.S.A. He completed his Bachelor of Science in Pre-Medicine from 1974-1977 and his Doctor of Medicine degree from the University of the Philippines College of Medicine, Manila from 1977-1981. He performed a traditional rotating Clinical Internship at the University of the Philippines-Philippine General Hospital Medical Center, Manila, Philippines from 1981-1982. After fulfilling his government service requirement in 1987, he accepted a Predoctoral Fellowship for Ph.D. in Anatomy and Neuroscience at the Neuroscience Center of Excellence, University of Tennessee Health Science Center, Memphis. In 1988, he accepted a Postdoctoral Research Fellowship in Cell Biology in the laboratory of Ruth Caldwell, Ph.D. at the Medical College of Georgia, Augusta Georgia. He was promoted to Instructor of Cell Biology and Anatomy in 1991 after successfully competing for a National American Heart Association Research Fellowship. In 1992, he obtained his first regular faculty position in the U.S. as an Assistant Professor of Cell Biology and Genetics at the University of North Texas Health Science Center in Fort Worth, Texas. He was promoted to Associate Professor of Cell Biology and Genetics in 1998. He later served as Department Graduate Student Advisor from 2000-2004, Department Vice-Chair from 2004-2007. From 2000-2007, he was concurrently the Director of Gross Anatomy. In 2008, Dr. Roque moved to Touro University Nevada in Henderson, Nevada as Professor of Basic Sciences and Director of Gross Anatomy, and founded the Medical Health Sciences Program at Touro University Nevada, serving as its first Director.